



Contents lists available at ScienceDirect

Journal of Colloid and Interface Science

www.elsevier.com/locate/jcis



Preparation of highly fluorescent magnetic nanoparticles for analytes-enrichment and subsequent biodetection

Bingbo Zhang^{a,*}, Bingdi Chen^a, Yilong Wang^a, Fangfang Guo^a, Zhuoquan Li^a, Donglu Shi^{a,b}

^aThe Institute for Advanced Materials & Nano Biomedicine, Tongji University, Shanghai 200092, China

^bSchool of Energy, Environmental, Biological and Medical Engineering, University of Cincinnati, Cincinnati, OH 45221-0012, USA

ARTICLE INFO

Article history:

Received 12 August 2010

Accepted 28 September 2010

Available online 25 October 2010

Keywords:

Fluorescent magnetic nanoparticles

Quantum dots

Magnetic

Silica

Flow cytometric analysis

ABSTRACT

Bifunctional nanoparticles with highly fluorescence and decent magnetic properties have been widely used in biomedical application. In this study, highly fluorescent magnetic nanoparticles (FMNPs) with uniform size of ca. 40 nm are prepared by encapsulation of both magnetic nanoparticles (MNPs) and shell/core quantum dots (QDs) with well-designed shell structure/compositions into silica matrix via a one-pot reverse microemulsion approach. The spectral analysis shows that the FMNPs hold high fluorescent quantum yield (QY). The QYs and saturation magnetization of the FMNPs can be regulated by varying the ratio of the encapsulated QDs to MNPs. Moreover, the surface of the FMNPs can be modified to offer chemical groups for antibody conjugation for following use in target-enrichment and subsequent fluorescent detection. The *in vitro* immunofluorescence assay and flow cytometric analysis indicate that the bifunctional FMNPs-antibody bioconjugates are capable of target-enrichment, magnetic separation and can also be used as alternative fluorescent probes on flow cytometry for biodetection.

© 2010 Elsevier Inc. All rights reserved.

1. Introduction

Multifunctional nanoparticles are attracting more and more attentions of material scientists, chemists and biologists, since such multifunctional particles combine multiple properties and have various applications [1–5]. Especially, considerable efforts have been devoted to design fluorescent magnetic nanoparticles (FMNPs) with both fluorescence and magnetism functionalities for potential application as dual-modality imaging probes [6–11]. In addition to the use as imaging probes, FMNPs have potential applications in bio-analysis [12,13]. FMNPs can be employed to separate and enrich the analytes from complicated samples, and then the enriched analytes can be detected with the fluorescent signal generated by FMNPs. The preparations of FMNPs have been extensively reported these years [14–18]. However, one of the common problems during the preparation of FMNPs is fluorescent quenching, resulting in the low QY of FMNPs [15,19]. The fluorescent quenching is mainly owing to two factors. The first one is the photo/chemical stability of the used fluorophores. FMNPs are usually prepared and used in the complicated chemical solution, and many chemicals could be the quencher of fluorophores [20–24]. The second factor is the influence of MNPs because of the strong absorption cross section of the magnetic nanoparticles [15] and the possible energy transfer between fluorophores and MNPs [25]. The second quenching effect could be weakened by adjusting

the mol ratio of embedded fluorophores to MNPs [17]. However, the saturation magnetization of the FMNPs will be insufficient if the ratio of MNPs to fluorophores is too low. Thus, the most promising solution to solve fluorescent quenching is the selection of proper fluorophores.

Semiconductor nanocrystals called QDs [26] have high photostability, high emission quantum yield, narrow emission peaks, size-dependent wavelength tunability in comparison with organic dyes and fluorescent proteins, which make them more interesting for potential biomedical application [27]. Most of QDs are hydrophobic, since they are capped by organic ligands. And they are photo stable in organic solution. However, hydrophobic QDs should be transferred into hydrophile for biomedical application. One of the most widely used modification methods is silanization. However, the fluorescence of QDs will be quenched in various degrees when they are transferred into water phase [28,29]. Our group has done some work about the changes of optical property of QDs before and after silica-coating. And study data indicated that QDs with appropriate structure and composition of shells can retain the initial QY more efficiently after silanization [30]. Based on the results from our past work, in this study, the well-designed seven layered shell/core QDs (CdSe/CdS/CdS/Cd_{0.75}Zn_{0.25}S/Cd_{0.5}Zn_{0.5}S/Cd_{0.25}Zn_{0.75}S/ZnS/ZnS) were selected to prepare highly fluorescent FMNPs with the classical silica-coating via the reverse microemulsion approach [31]. After the successful preparation of FMNPs, the prepared samples were chemically-activated by amino groups for antibody-labeling and the following target-enrichment and subsequent fluorescent detection on a flow cytometry.

* Corresponding author. Fax: +86 21 65983706 819.

E-mail address: bingbozhang@tongji.edu.cn (B. Zhang).

2. Materials and methods

2.1. Materials

Selenium powder (100 mesh, 99.99%, Aldrich), cadmium oxide (CdO, 99.5%, Aldrich), zinc oxide (ZnO, 99.9%, Sigma), Fe(acac)₃ (Alfa Aesar), 1,2-hexadecanediol (Alfa Aesar), benzyl ether (Alfa Aesar), sulphur (99.98%, Aldrich), tri-*n*-butylphosphine (TBP, 90%, TCI, Japan), tri-*n*-octylphosphine oxide (TOPO, 90%, Aldrich), octadecylamino (ODA, 90%, ACROS), 1-octadecene (ODE, 90%, ACROS), oleic acid (OA, 90%, Aldrich), Carboxyl-polystyrene (PS) microspheres (Tianjin BaseLine ChromTech Research Center); Bovine Serum Albumin (BSA), human IgG: purified total IgG from normal human serum, in which heavy chain is 50,000 Da, light chain is 25,000 Da. Goat anti-human IgG: pure human total IgG immune against goat until 1:100,000 (ELISA), above supplied by BEIJING DINGGUO BIOTECHNOLOGY CO. Ltd. 1-Ethyl-3-(3-dimethylaminopropyl) carbodiimide hydrochloride (EDC, GL Biochem (Shanghai) Ltd.), 3-aminopropyltriethoxysilane (APTES, Alfa Aesar), NP-40 (Fluka), TEOS, aqueous ammonia solution (25 wt.%), cyclohexane, glutaraldehyde, acetone, and argon (oxygen free) were obtained from local suppliers. All chemicals were used without further purification.

2.2. Synthesis of TOPO-capped bare/core CdSe QDs and shell/core QDs

Bare/core QDs were synthesised according to a previously reported protocols with minor modifications [32,33]. Briefly, 0.3 mmol of CdO, 0.4 mL of OA, 4.0 mL of ODE were loaded into a 50 mL flask. First, the mixture was heated to 300 °C under an Ar flow, and CdO was dissolved to generate a colorless homogeneous solution. Next, the solution was cooled to room temperature (RT), and then 2.50 g ODA and 0.50 g TOPO were added into the flask. Then the system was heated again to 280 °C under an Ar flow. After that, a selenium solution (1.8 mmol of Se powder dissolved in 2 mL of TBP) was injected quickly. Following the injection of selenium, nanocrystals were grown at 260 °C for different amounts of time depending on the desired sizes, and the solution underwent color changes from colorless, to green, to yellow and finally to red, which is the indication of QDs formation. Next, the solution was injected into chloroform. The TOPO-capped QDs were precipitated by adding dry ethanol, collected by centrifugation, washed with methanol several times, and vacuum dried for use. A typical synthesis of shell/core QDs was performed as follows: CdSe nanocrystals dissolved in 10 mL of hexane were mixed with 1.5 g of ODA and 5.0 g of ODE in a 25 mL three-neck flask. Then, the flask was switched to Ar flow to replace the air for 30 min, and then heated to 100 °C for another 5–10 min to remove hexane from the system. Subsequently, the reaction mixture was further heated to 240 °C for the injections. The procedures of Cd, Zn and S resource injections were according to Ref. [33]. The final product was diluted by hexane that was followed by a methanol extraction, or acetone precipitation of the nanocrystals. Excess aminos were further removed by dissolving the nanocrystals in chloroform and precipitating them with acetone. In this paper, seven layered shell/core QDs were prepared. The structure and compositions were CdSe/CdS/CdS/Cd_{0.75}Zn_{0.25}S/Cd_{0.5}Zn_{0.5}S/Cd_{0.25}Zn_{0.75}S/ZnS/ZnS (7Layers) with QY of 47.8%. For comparison, other shell/core QDs were prepared. And the shell structure and compositions were CdSe/CdS/CdS/CdS (QY, 43.5%) and CdSe/ZnS/ZnS/ZnS (QY, 50.8%).

2.3. Synthesis of MNPs

Fe₃O₄ MNPs were synthesised with minor modifications according to a previously published procedure [34]. Fe (acac)₃ (1 mmol),

1,2-hexadecanediol (6 mmol), oleic acid (4 mmol), oleylamino (3 mmol), and benzyl ether (12 mL) were mixed and magnetically stirred under a flow of nitrogen. The mixture was heated to 200 °C for 2 h and then heated to reflux (300 °C) for 1 h. The black-colored mixture was cooled to RT by removing the heat source. Under ambient conditions, ethanol (20 mL) was added to the mixture, and a black material was precipitated and separated via centrifugation.

2.4. Synthesis of FMNPs

FMNPs were synthesised according to a previously published procedure with minor modifications [31]. Typically, 10 mL of cyclohexane, 1.3 mL of NP-40, 200 μL of QDs (3.3 × 10⁻⁶ M) stock solution in chloroform, 100 μL of MNPs in chloroform (5 mg/mL), and 120 μL of TEOS were added into a flask under vigorous stirring. Thirty minutes after the microemulsion system was formed, 100 μL of ammonia aqueous solution (25 wt.%) was introduced to initiate the polymerization process. The silica growth was completed after 24 h of stirring at RT. Chemically-activated silica-coated nanoparticles were prepared by adding 20 μL APTES for the introduction of NH₂ group into above reaction system after 24 h polymerization. The resulting nanoparticles were isolated from the microemulsion using acetone and ethanol four times to remove any surfactant and unreacted molecules.

2.5. Covalent immobilization of antibody and antigen onto FMNPs surface and carboxylated PS microspheres respectively

The goat anti-human IgG antibody was directly immobilized onto the FMNPs with well-established glutaraldehyde method shown below. (1) Fluorescent FMNPs 10 mg was dispersed into the 1.0 mL phosphate buffered saline (PBS) buffer containing 5% glutaraldehyde for about 2 h at RT. (2) The nanoparticles were separated by centrifugation and washed with PBS three times. After the nanoparticles were redispersed in PBS, they were further incubated with IgG antibody (10.0 mg) for 3 h at RT with gentle shaking. (3) The antibody-labeled FMNPs were washed with PBS several times to remove excess IgG antibody and kept at 4 °C in PBS (0.01 M, pH 7.2, 0.5% BSA). Highly carboxylated PS microspheres were coated with human IgG (as positive control) and BSA (as negative control) via the covalent bonds between human IgG molecules and microspheres. The solutions of IgG or BSA (5.0 mg), EDC (10.0 mg) and microspheres (10.0 mg) were gently mixed in the PBS buffer for 2 h at RT using an orbital shaker followed by storage at 4 °C.

2.6. In vitro target-enrichment, magnetic separation and flow cytometric analysis with antibody-labeled FMNPs

The immunofluorescence assay for the positive and negative control experiments were both carried out in the same manner. The IgG-coated PS microspheres (2.0 mg/mL, 1.0 mL) were firstly blocked for 30 min at RT in the PBS-BSA buffer (0.01 M, pH7.2, 0.5% BSA), then gently mixed with anti-human IgG labeled FMNPs bioconjugates (20 nmol/L, 0.1 mL) using an orbital shaker at RT. After 30 min, external magnetic field was applied to enrich and following separate microsphere-FMNPs bioconjugates. Finally the captured microspheres were first examined under an OLYMPUS.BX51 fluorescence microscope equipped with an OLYMPUS MICRO DP 70 camera and a broad band light source (ultraviolet 330–385 nm). The illumination light was from an O-LH100HG 100 W mercury lamp with automatic exposure control. And then the positive and negative microspheres treated with anti-human IgG labeled FMNPs were analyzed on the flow cytometry.

2.7. Characterization techniques

Ultraviolet–visible (UV–vis) absorption spectra were recorded on a UV-2450 spectrophotometer (SHIMADZU). Photoluminescence (PL) measurement was performed at RT using an F-4500 (HITACHI) spectrophotometer. QDs, MNPs and FMNPs were visualized using a Tecnai G² F20 TEM operating at an acceleration voltage of 200 kV. The dispersion property of the FMNPs in solution was measured using a particle size analyzer (Nano ZS, Malvern). The fluorescence QY of the QDs were carefully measured using Rhodamin 6G as fluorescence standard. Fourier transform infrared spectroscopy (FTIR) spectra were recorded on a Bio-Rad FTS 6000 spectrometer at room temperature. The digital fluorescent photos of FMNPs were taken with a digital camera. The magnetic property of FMNPs was analyzed at Vibrating Samples Magnetometer, LDJ9600-1. The flow cytometric analysis was carried out using a BD FACS Calibur flow cytometry (BD Biosciences, Franklin lakes, USA).

3. Results and discussion

The morphology and structure of the QDs, MNPs and the as-prepared FMNPs were characterized by TEM (Fig. 1). The hydrophobic MNPs and QDs showed array distribution on the copper grids in Fig. 1A and B respectively, and the FMNPs were uniform in size of about 40 nm (Fig. 1C). The dispersion property and hydrodynamic size of the FMNPs in solution was tested by a particle size analyzer (Fig. 2). The result showed the as-prepare FMNPs was about 40 nm, which is identical to that of TEM characterization. And the size distribution is narrow, which is very important for biomedical use.

As fluorescent probes for the biodetection, the QY of the probes should be high enough that will enhance the sensitivity of detection. Researchers have done some work to improve the QY of water-soluble QDs [35–37]. Although silanization of QDs is the most popular strategy for water-solubilization, the QY of silica-coated QDs probes is not as high as expectation since the original QDs are not stable enough for water-solubilization, especially hydrophobic CdSe bare/core QDs. The bare/core QDs have more cavities and dangling bonds than that of shell/core QDs [38]. The electrons generated from the bare/core QDs can be trapped in cavities and captured by the dangling bonds on the surface. Thus, this kind of QDs is render to quenching during water-solubilization.

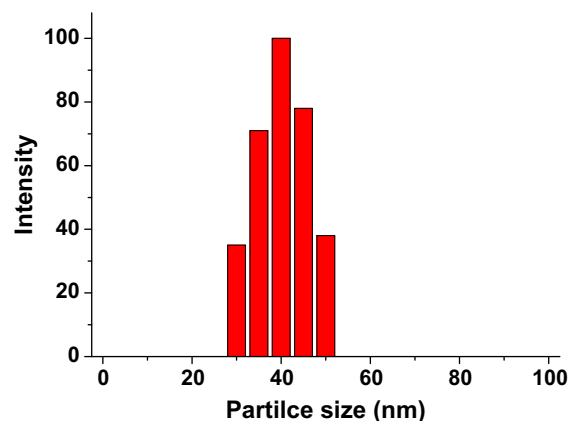


Fig. 2. Size distribution of amino-FMNPs in deionized water measured by the particle size analyzer.

Shell/core QDs would be much better than that of bare/core QDs against fluorescent quenching. However, not all kinds of shell/core QDs are well photo stable against phase-transferring. And our past work addressed that the construction of multi-shells around the cores and proper compositions in each shell are critical to the maintenance of QY during the phase-transferring [30]. In the present work, co-encapsulation of QDs with MNPs into silica matrix has the same facts that shell and composition of the used QDs will influence the QY of FMNPs extensively. Furthermore, the black and photon absorption-like MNPs will further affect the fluorescence emission. In this study, the PL of shell/core QDs of CdSe/ZnS/ZnS with and without MNPs were both completely quenched after silica-encapsulation, as shown in Fig. 3A. In comparison, the shell/core QDs of CdSe/CdS/CdS/CdS, where CdS replaced the ZnS hold about half of the original QY when they were coated by silica. However, their PL was nearly quenched when being encapsulated with MNPs (Fig. 3B). The results indicated that the QY of QDs with CdS shell is higher than that of QDs with ZnS shell after silica-coating. Based on this experimental results and our past research results, herein, well-designed seven layered shell/core QDs, namely, CdSe/CdS/CdS/Cd_{0.75}Zn_{0.25}S/Cd_{0.5}Zn_{0.5}S/Cd_{0.25}Zn_{0.75}S/ZnS/ZnS were chosen for the preparation of FMNPs as the fluorescent moiety. Elemental analysis and XRD

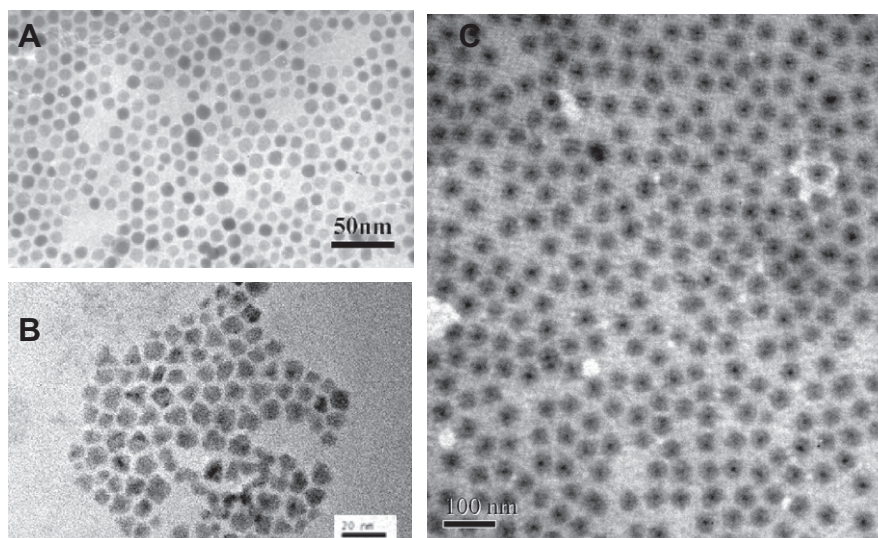


Fig. 1. TEM images of (A) hydrophobic MNPs, (B) hydrophobic seven layered shell/core QDs and (C) FMNPs.

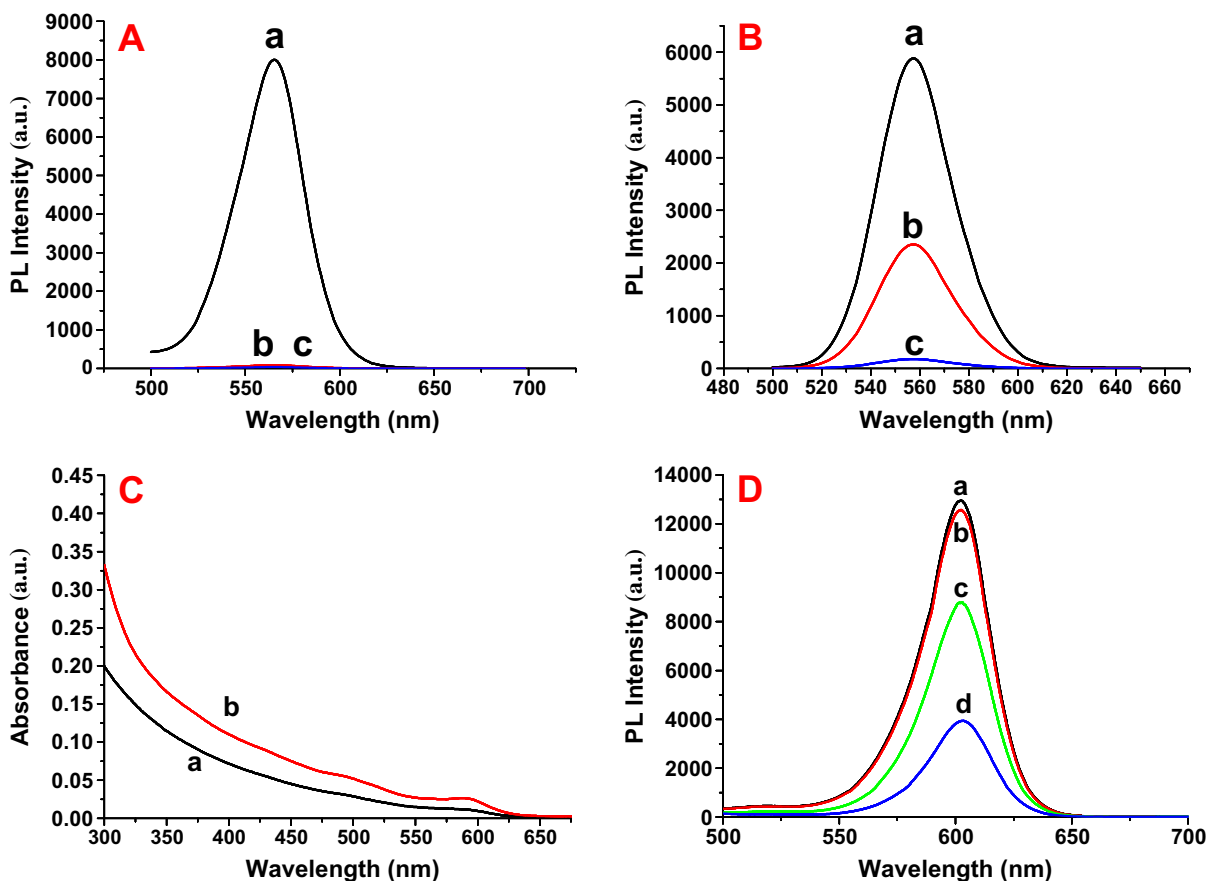


Fig. 3. The changes of PL intensity of FMNPs with three different types of QDs. (A) the QDs were CdSe/ZnS/ZnS/ZnS (a, hydrophobic QDs in cyclohexane; b, after silica-coating; c, FMNPs with 100 μ L of such QDs and 100 μ L of MNPs); (B) the QDs were CdSe/CdS/CdS/CdS (a, hydrophobic QDs in cyclohexane; b, after silica-coating; c, FMNPs with 100 μ L of such QDs and 100 μ L of MNPs); (C) the UV-vis spectrum of (a) FMNPs and (b) hydrophobic QDs; (D) the varying PL intensity of (a) 100 μ L hydrophobic QDs in cyclohexane, (b) silica coated 100 μ L of QDs, (c) FMNPs with 100 μ L of QDs and 100 μ L of MNPs, (d) FMNPs with 100 μ L of QDs and 200 μ L of MNPs. The seven layered of CdSe/CdS/CdS/Cd_{0.75}Zn_{0.25}S/Cd_{0.5}Zn_{0.5}S/Cd_{0.25}Zn_{0.75}S/ZnS/ZnS were used in (C) and (D).

data showed the difference between core and shell/core QDs, as shown in Supplementary Figs. S1 and S2.

UV-vis spectroscopy was used to monitor the optical property changes of the well-designed seven layered shell/core QDs before and after silica-encapsulation (Fig. 3C). The characteristic absorbance of QDs was not as distinct and sharp after being coated compared to that of hydrophobic QDs dissolved in chloroform. It is likely that absorption due to light scattering from the silica particles made the absorption features appear less sharp for the QDs [39]. The mol ratios of QDs to MNPs in silica nanoparticles affect the PL intensity (or QY) of the resulting FMNPs. Furthermore, MNPs could act as a photon absorber from QDs nearby, which will decrease the QY of the as-prepared FMNPs. In this study, the seven layered QDs retained its original QY after silica-encapsulation, verifying the good resistance to quenching of the well-designed shell/core QDs. And when the seven layered QDs and MNPs were both encapsulated into silica, the result showed that the as-prepared FMNPs with 33.3% of QY containing 100 μ L of QDs (3.3×10^{-6} M) and 100 μ L of MNPs (5 mg/mL) remained over half of the initial QY of QDs (47.8%). Three different QDs/MNPs ratios were used to monitor the changes of PL intensity (or QY) of FMNPs (Fig. 3D). The behaviors of resistance to quenching of FMNPs vary with the shell structure and composition of the used QDs. The results indicated that the CdS shell play an important role for QY-retainment since the lattice mismatch between CdSe and CdS is lower than that of CdSe and ZnS. And multi-shells QDs are better than core or single shell QDs in the aspect of anti-quenching.

The magnetic property of FMNPs was analyzed with vibrating sample magnetometer (VSM) as shown in Fig. 4. The saturation magnetization values of the FMNPs were 2.6 emu/g at 300 K. The

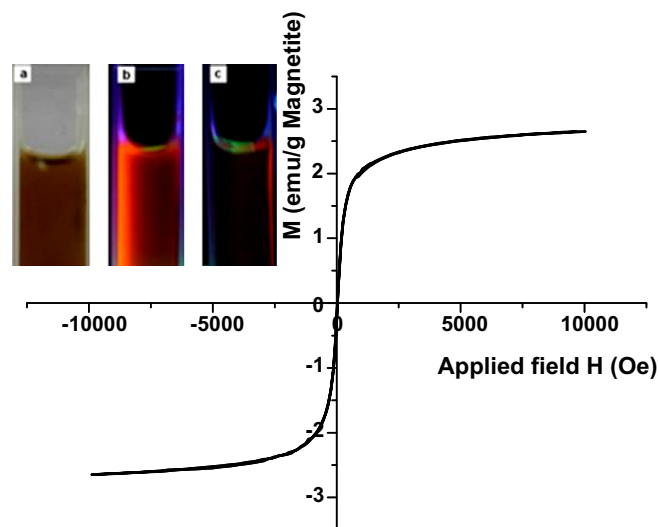


Fig. 4. VSM of FMNPs with the inset showing the digital images of FMNPs: (a) under daylight, (b and c) under a portable UV lamp irradiation. (a and b) Without magnet, (c) magnetic separation using an external magnet.

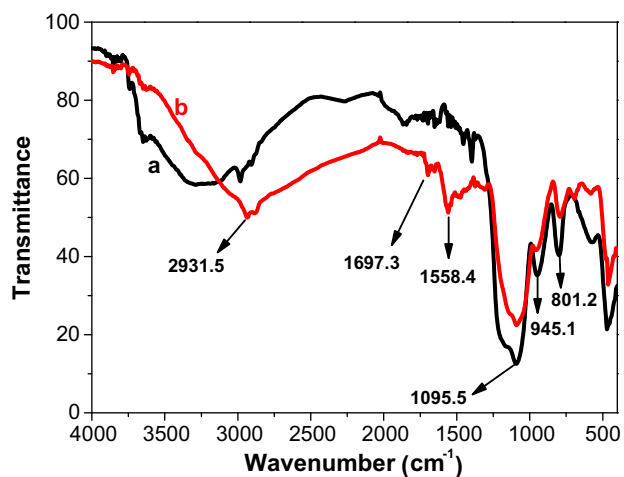


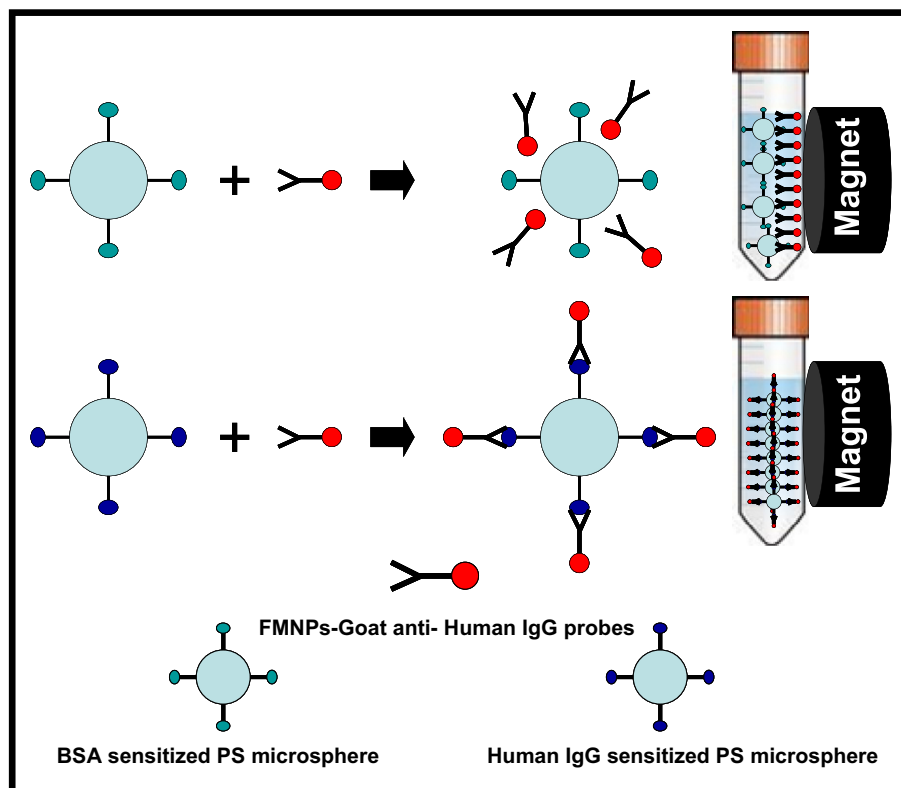
Fig. 5. FTIR spectra of FMNPs (a) and amino-FMNPs (b).

magnetic remanence of the sample was nearly zero and that means the synthesised FMNPs exhibited superparamagnetism, which favors the redispersion of FMNPs after the external magnetic field is removed. Fig. 4 inset showed that there was no fluorescence emission in DI water away from the magnet, while on the right wall (close to magnet) of colorimetric tube emitted bright fluorescence, which indicated that the QDs and MNPs had been both embedded into FMNPs.

The unmodified FMNPs with hydroxyl are difficult to conjugate with biomolecules. Thus, the introduction of active chemical groups, such as amino, thiol and carboxyl, is important. In this study, 3-aminopropyltriethoxysilane (APTES) which contains primary amino was added into the reaction system after 24 h of

silica-polymerization. Fig. 5 showed the FTIR spectra of FMNPs and amino modified FMNPs. Bands at 1095.5 cm^{-1} , 945.1 cm^{-1} and 801.2 cm^{-1} in the two spectra confirmed the formation of silica. And bands at 2931.5 cm^{-1} in the spectra of Fig. 5b was from the methylene groups of APTES, while the characteristic bands at $1697.3/1558.4\text{ cm}^{-1}$ also indicated the successful introduction of amino groups onto the surface of FMNPs. Furthermore, zeta potential of FMNPs was measured to monitor the potential changes after group-introduction. The negatively charged FMNPs with -48.32 mV turned positive (26.63 mV) after amino was introduced.

The prepared amino-FMNPs were labeled with goat anti-human IgG as the specific fluorescent magnetic probes. The Scheme 1 showed the illustration of *in vitro* target-enrichment and the following magnetic separation based on the FMNPs probes. The enriched specific PS microspheres were collected and then examined under the fluorescent microcopy (Fig. 6A and B). The immunofluorescence exam showed the fluorescence on the positive control microspheres was obviously brighter in Fig. 6B, while nearly no fluorescent signal on the surface of negative control microspheres in Fig. 6A, which was well consistent with our expectation. The positive and negative microspheres were then characterized under a flow cytometry. As shown in Fig. 6C and D, the data indicated more than 98% human IgG sensitized PS microspheres were captured by the anti-human IgG labeled FMNPs. And the fluorescent intensity from the human IgG sensitized PS microspheres is much higher than that of BSA sensitized PS microspheres. This result was identical with that of *in vitro* particle-based immunofluorescence assays (Fig. 6A and B). Although planar assays based on flat carriers (glass slides, flat-bottomed ELISA plate) are among the most intensively investigated for bioassays [40], suspension array based on particles is more promising since its inherent and unique characteristics. The high binding capacity of three-dimensional microspheres makes the suspension array a very sensitive platform for immunofluorescence assays. One of the most used carriers in



Scheme 1. Schematic diagram of *in vitro* target-enrichment and magnetic separation under an external magnet based on the same single antibody-labeled FMNPs.

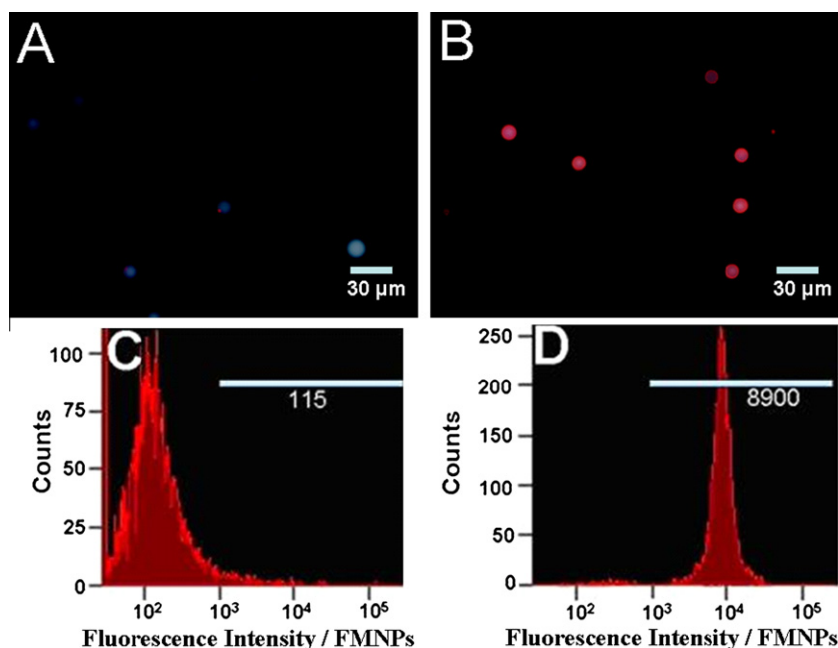


Fig. 6. The immunofluorescence images of BSA (A, negative control) and human IgG (B, positive control) sensitized PS microspheres treated with FMNPs-anti-human IgG probes; flow cytometric analysis of PS microspheres when treated with FMNPs-anti-human IgG probes for 0.5 h. In control experiments, BSA sensitized PS microspheres was used (C), while human IgG sensitized PS microspheres were used as the positive control (D). The mean fluorescence intensity of FMNPs labeled PS microspheres was noted below the line. The positively labeling PS microspheres were defined as the fluorescence value $>10^3$.

suspension array is particle or bead. They have great potentials for bioapplication, for example, being integrated with a flow cytometric system [41], or Luminex flow analyzer [42] to make a high-throughput screening. In this study, carboxyl-PS microspheres were used to be the solid supports for immobility of antigen, and the bifunctional FMNPs were used as the both of capture and fluorescent detecting probes. The results indicated the antibody-labeled FMNPs can specifically capture and separate the corresponding microspheres, and then the resulting enriched microsphere-FMNPs bioconjugates can be also successfully analysed on the flow cytometry with the help of fluorescent moiety of FMNPs. The target-enrichment step can concentrate the rare analytes from samples, which is critical to the biochemical analysis. And superparamagnetic micro/nano particles are usually and successfully used in the magnetic enrichment and separations. In this study, superparamagnetic and fluorescent were integrated within a single nanoparticle. Such kind of nanoparticles could offer more convenience for biochemical analysis in comparison with that of individual magnetic particles and fluorescent probes.

4. Summary

Highly uniform fluorescent magnetic nanoparticles are prepared by encapsulation of both MNPs and proper type of QDs into silica matrix via a one-pot reverse microemulsion approach. QDs with well-designed seven layered shell/core QDs are chosen for the fluorescent moiety of the FMNPs. Varying characterizations show that the as-prepared FMNPs had uniform size (less than 50 nm), nice optical properties, and decent saturation magnetization. The as-obtained FMNPs are easily modified with amino groups for the following antibody-labeling. The subsequent *in vitro* experiments indicate that the antibody-FMNPs probes had strong target-capture and enrichment ability because of its targeting specificity and magnetic responsiveness. And the flow cytometric analysis suggests that the as-prepared FMNPs can be also used as fluorescent probes, thanks to the highly stable fluores-

cent FMNPs. In this study, both the target-enrichment process and fluorescent detection step can be accomplished by the same single bifunctional FMNPs, which will be more convenient and time-reducing for biochemical analysis.

Acknowledgments

This work was supported by the National Natural Science Foundation of China (51003078), the National High Technology Program (2008AA09Z111) and Program for Young Excellent Talents in Tongji University (2009KJ072) and the Opening Project of MOE Key Laboratory of Analytical Chemistry for Life Science, Nanjing University (KLACLS1001).

Appendix A. Supplementary material

Supplementary data associated with this article can be found, in the online version, at [doi:10.1016/j.jcis.2010.09.084](https://doi.org/10.1016/j.jcis.2010.09.084).

References

- [1] S. Santra, C. Kaittanis, J. Grimm, J.M. Perez, *Small* 5 (2009) 1862.
- [2] Z. Shi, K.G. Neoh, E.T. Kang, B. Shuter, S.C. Wang, *Contrast Media Mol. Imaging* 5 (2010) 105.
- [3] J. Bao, W. Chen, T. Liu, Y. Zhu, P. Jin, L. Wang, J. Liu, Y. Wei, Y. Li, *ACS Nano* 1 (2007) 293.
- [4] R. Koole, W.J. Mulder, M.M. van Schooneveld, G.J. Strijkers, A. Meijerink, K. Nicolay, *Wiley Interdiscip. Rev. Nanomed. Nanobiotechnol.* 1 (2009) 475.
- [5] W. Hwang do, I.C. Song, D.S. Lee, S. Kim, *Small* 6 (2010) 81.
- [6] C.W. Lu, Y. Hung, J.K. Hsiao, M. Yao, T.H. Chung, Y.S. Lin, S.H. Wu, S.C. Hsu, H.M. Liu, C.Y. Mou, C.S. Yang, D.M. Huang, Y.C. Chen, *Nano Lett.* 7 (2007) 149.
- [7] H. Gu, R. Zheng, X. Zhang, B. Xu, *J. Am. Chem. Soc.* 126 (2004) 5664.
- [8] L. Li, H. Li, D. Chen, H. Liu, F. Tang, Y. Zhang, J. Ren, Y. Li, *J. Nanosci. Nanotechnol.* 9 (2009) 2540.
- [9] J. Cheon, J.H. Lee, *Acc. Chem. Res.* 41 (2008) 1630.
- [10] W.J. Mulder, A.W. Griffioen, G.J. Strijkers, D.P. Cormode, K. Nicolay, Z.A. Fayad, *Nanomedicine (Lond.)* 2 (2007) 307.
- [11] L.E. Jennings, N.J. Long, *Chem. Commun. (Camb.)* (2009) 3511.
- [12] A. Quarta, R. Di Corato, L. Manna, A. Ragusa, T. Pellegrino, *IEEE Trans. Nanobiosci.* 6 (2007) 298.

- [13] G. Wang, P. Xie, C. Xiao, P. Yuan, X. Su, J. Fluoresc. 20 (2010) 499.
- [14] S.T. Selvan, P.K. Patra, C.Y. Ang, J.Y. Ying, Angew Chem., Int. Ed. Engl. 46 (2007) 2448.
- [15] S.K. Mandal, N. Lequeux, B. Rotenberg, M. Tramier, J. Fattaccioli, J. Bibette, B. Dubertret, Langmuir 21 (2005) 4175.
- [16] Z.Q. Tian, Z.L. Zhang, J. Gao, B.H. Huang, H.Y. Xie, M. Xie, H.D. Abruna, D.W. Pang, Chem. Commun. (Camb.) (2009) 4025.
- [17] B. Zhang, J. Cheng, X. Gong, X. Dong, X. Liu, G. Ma, J. Chang, J. Colloid Interface Sci. 322 (2008) 485.
- [18] R. Kas, E. Sevinc, U. Topal, H.Y. Acar, J. Phys. Chem. C 114 (2010) 7758.
- [19] N. Hirata, K. Tanabe, A. Narita, K. Tanaka, K. Naka, Y. Chujo, S. Nishimoto, Bioorg. Med. Chem. 17 (2009) 3775.
- [20] H.Z. Zheng, L. Liu, Z.J. Zhang, Y.M. Huang, D.B. Zhou, J.Y. Hao, Y.H. Lu, S.M. Chen, Spectrochim. Acta A 71 (2009) 1795.
- [21] M. Ogawa, N. Kosaka, M.R. Longmire, Y. Urano, P.L. Choyke, H. Kobayashi, Mol. Pharm. 6 (2009) 386.
- [22] J. Widengren, A. Chmyrov, C. Eggeling, P.A. Lofdahl, C.A. Seidel, J. Phys. Chem. A 111 (2007) 429.
- [23] H. Chen, S.S. Ahsan, M.B. Santiago-Berrios, H.D. Abruna, W.W. Webb, J. Am. Chem. Soc. 132 (2010) 7244.
- [24] C. Dong, X. Huang, J. Ren, Ann. N.Y. Acad. Sci. 1130 (2008) 253.
- [25] E. Oh, M.Y. Hong, D. Lee, S.H. Nam, H.C. Yoon, H.S. Kim, J. Am. Chem. Soc. 127 (2005) 3270.
- [26] A.P. Alivisatos, Science 271 (1996) 933.
- [27] W.C. Chan, D.J. Maxwell, X. Gao, R.E. Bailey, M. Han, S. Nie, Curr. Opin. Biotechnol. 13 (2002) 40.
- [28] D. Dorokhin, N. Tomczak, M. Han, D.N. Reinhoudt, A.H. Velders, G.J. Vancso, ACS Nano 3 (2009) 661.
- [29] W. Sheng, S. Kim, J. Lee, S.W. Kim, K. Jensen, M.G. Bawendi, Langmuir 22 (2006) 3782.
- [30] B.B. Zhang, X.Q. Gong, L.J. Hao, J. Cheng, Y. Han, J. Chang, Nanotechnology 19 (2008).
- [31] M. Darbandi, R. Thomann, T. Nann, Chem. Mater. 17 (2005) 5720.
- [32] Z.A. Peng, X. Peng, J. Am. Chem. Soc. 123 (2001) 183.
- [33] J.J. Li, Y.A. Wang, W. Guo, J.C. Keay, T.D. Mishima, M.B. Johnson, X. Peng, J. Am. Chem. Soc. 125 (2003) 12567.
- [34] S. Sun, H. Zeng, D.B. Robinson, S. Raoux, P.M. Rice, S.X. Wang, G. Li, J. Am. Chem. Soc. 126 (2004) 273.
- [35] Q. Wang, Y.C. Kuo, Y.W. Wang, G. Shin, C. Ruengruglikit, Q.R. Huang, J. Phys. Chem. B 110 (2006) 16860.
- [36] H. Peng, L.J. Zhang, C. Soeller, J. Travas-Sejdic, J. Lumin. 127 (2007) 721.
- [37] J.H. Wang, H.L. Zhang, Y.Q. Li, J.R. Qian, H.Q. Wang, T.T. Xu, Y.D. Zhao, J. Nanopart. Res. 12 (2010) 1687.
- [38] M.A. Hines, P. Guyot-Sionnest, J. Phys. Chem. – US 100 (1996) 468.
- [39] M. Han, X. Gao, J.Z. Su, S. Nie, Nat. Biotechnol. 19 (2001) 631.
- [40] P. Mitchell, Nat. Biotechnol. 20 (2002) 225.
- [41] J.P. Nolan, L.A. Sklar, Trends Biotechnol. 20 (2002) 9.
- [42] A. Clavijo, K. Hole, M.Y. Li, B. Collignon, Vaccine 24 (2006) 1693.